Biophys Rep 2019, 5(5–6):219–234
https://doi.org/10.1007/s41048-019-00094-7

Biophysics Reports

OPINION

Towards understanding the mechanisms of proton pumps in Complex-I of the respiratory chain

Xuejun C. Zhang[1,2]✉, **Bin Li**[1,2]

[1] National Laboratory of Biomacromolecules, CAS Center for Excellence in Biomacromolecules, Institute of Biophysics, Chinese Academy of Sciences, Beijing 100101, China
[2] College of Life Science, University of Chinese Academy of Sciences, Beijing 100049, China

Received: 15 April 2019 / Accepted: 7 July 2019 / Published online: 1 October 2019

INTRODUCTION

Complex-I (*i.e.,* nicotinamide adenine dinucleotide (NADH):ubiquinone (quinone or Q) oxidoreductase) of the respiratory chain is crucial for converting energy from its redox form (*i.e.,* electron transfer) to the transmembrane electrochemical potential (Hirst 2013; Kaila 2018; Verkhovskaya and Bloch 2013; Walker 1992). Homologs of Complex-I are ubiquitously expressed throughout all forms of life, from bacteria to human cells (Friedrich and Scheide 2000). Complex-I utilizes the redox energy of the NADH-quinone pair to drive four protons across the membrane (Jones *et al.* 2017). In both the bacteria cytoplasmic membrane as well as the mitochondrial inner membrane, the electrochemical potential of protons (*i.e.,* proton-motive force, PMF) established by Complex-I is found to be always in an inside-alkaline and inside-negative orientation. The energy conversion catalyzed by Complex-I is highly efficient, and under near-equilibrium conditions, the process is thermodynamically reversible, characterized by negligible loss of energy through heat. This high efficiency indicates that the redox reaction is tightly coupled to the process of transmembrane-vectorial proton translocation (Hirst 2013; Verkhovskaya and Bloch 2013; Vinogradov 1998).

Complex-I is the largest enzyme assembly among the five major complexes of the respiratory chain and represents the most sophisticated assembly of proteins among all the known transporter systems (Friedrich *et al.* 1995). Being the simplest member of the Complex-I family, the bacterial Complex-I is composed of 14 subunits and is considered to represent the core structure of the redox-driven proton-pumping machinery (Friedrich *et al.* 1995; Walker 1992). In addition to this core structure, the mitochondrial Complex-I consists of 30 or so supernumerary subunits probably playing roles in assembly, trafficking, stabilization, as well as regulation (Carroll *et al.* 2006; Friedrich and Scheide 2000). Structural biology studies have provided great insight into the three-dimensional (3D) structures of Complexes-I from a variety of species (Baradaran *et al.* 2013; Zhu *et al.* 2016; Zickermann *et al.* 2015). However, nearly all of the currently reported 3D structures of Complexes-I were determined in the absence of a negatively charged (semi-)quinone molecule, most likely representing the ground state (or even the deactivated state Kotlyar *et al.* 1992) of the complex.

Based on biochemical, biophysical, and structural biology analysis, the mechanisms of the electron transfer within the redox-enzyme component of Complex-I have been well established (recently reviewed in Ohnishi *et al.* 2018). In comparison, the mechanisms of the proton pumping in the membrane-spanning part of the complex remain under debate. Here, we discuss the current understanding of mechanisms in the framework of thermodynamics of general two-state transporters. On the basis of this analysis, we propose that Complex-I not only contains a set of antiporter-like subunits but also uses an antiporter-type mechanism for the energy coupling between the redox center and the proton pumps—a picture extended from a previously postulated single-stroke four-pump mechanism (Hirst 2013). In addition, we believe that the same understanding can

✉ Correspondence: zhangc@ibp.ac.cn (X. C. Zhang)

be applied to other types of (indirect) redox-driven proton pumps. The model proposed here represents our personal opinions and may not reflect the current mainstream beliefs of experts studying the biology of Complex-I.

OVERALL STRUCTURES OF COMPLEX-I

We will start with a brief description of the structures of Complex-I, focusing on their common features shared with other homologs. The bacterial Complex-I consists of two arms, namely the redox arm and the membrane arm, which are arranged in an L-shaped assembly (Guenebaut *et al.* 1998). Each arm contains seven subunits and ranges between 140 and 180 Å in length. We will refer to the crystal structure of the bacterial Complex-I (Baradaran *et al.* 2013; Efremov and Sazanov 2011), in particular the specific orientation shown in Fig. 1, as the reference for discussion on Complex-I structure (unless otherwise specified).

The hydrophilic redox arm of Complex-I, also referred to as its peripheral arm, protrudes into the cytoplasm. It transfers one pair of electrons from NADH to quinone. The NADH-binding site is located at the top of the redox arm, and the Q-binding site is supposedly formed in the junction region between the two long arms. Several redox prosthetic groups, including one flavin mononucleotide (FMN) and ~8 Fe–S clusters, are arranged along this redox arm. Together, they form an electron buffer zone between the NADH-redox center (also termed N-module) and quinone-redox center (Q-module) (Brandt 2011), with all prosthetic groups being reduced during steady-state turnover most of the time (Ohnishi *et al.* 2018). Based on the reported redox-potential values of these prosthetic clusters, the largest energy drop along the electron transfer pathway occurs between the membrane proximal Fe–S cluster (the so-called N2 site) and the Q-binding site (Ohnishi *et al.* 2018). (Here, for simplicity in our thermodynamic discussion, we refer to putative multiple Q-binding sites in the Q-model as just one single site.) This energy drop drives the vectorial translocation of substrate protons against their own electrochemical gradient. Importantly, both the long distance (~140 Å) between the N-module and Q-binding site and the obtuse angle (~120°) of the L-shaped complex minimize the disturbance of the NADH-redox reaction to the electrostatic field inside the membrane arm.

The hydrophobic membrane arm contains seven subunits (NuoA, H, and J–N, in the nomenclature of *Escherichia coli* Complex-I Friedrich *et al.* 1995). The four smaller subunits (NuoA, H, J, and K) proximal to the arm junction participate in formation of the Q-binding site and presumably of one proton pump, thus being referred to as proximal pump (P_P) module. The remaining three large subunits (NuoL, M, and N) are homologous to each other and to the Na^+/H^+ antiporter subunits of bacteria multiple resistance and pH-adaptation (Mrp) complex (Fearnley and Walker 1992; Hamamoto *et al.* 1994). Each of the three subunits is believed to function as a proton pump, and is therefore referred to as an antiporter-like, proton-pumping subunit. These three subunits are arranged along the membrane arm, and together are referred to as distal pump (P_D) module. During a functional cycle of Complex-I, each of the four pumps is thought to be responsible for translocation of one single proton across the membrane. Inside the membrane arm, a conserved central polar axis is formed by mixed acidic, basic, and

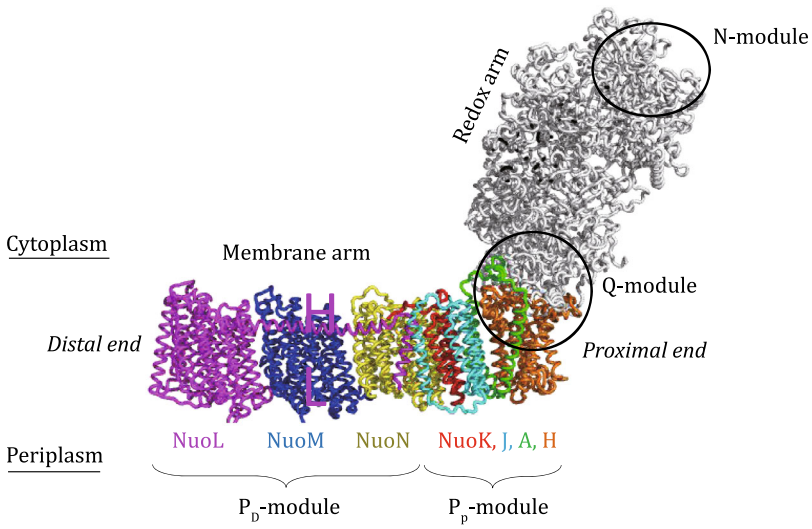

Fig. 1 Overall structure of Complex-I. Crystal structure of Complex-I from *Thermus thermophiles* (PDB ID: 4HEA) is shown in a tube diagram, with labels in the *E. coli* nomenclature consistent with those in the main text

other polar residues as well as probable bound water molecules, running through the entire arm (Baradaran *et al.* 2013). In addition, a "horizontal"/lateral (HL) long, nevertheless discontinuous, amphipathic helix (of ~75 amino acid residues) is extended from the distal subunit (NuoL) and contacts the other two antiporter-like subunits (NuoM and N) of the P_D-module, near the cytoplasmic surface of the membrane. In addition, at the bottom of the back side of the membrane arm, a series of β-hairpins and α-helices form another long amphipathic structural feature, termed βH-belt, near the periplasmic surface of the membrane. Both the HL helix and diagonally located βH-belt stabilize the long membrane arm, probably by restraining inter- and intra-subunit conformational changes, and may also function as storage apparatus of conformational energy. Previously, the HL helix was hypothesized to function as a piston to transmit mechanical energy from the Q-proximal end to the distal end of the membrane arm (Efremov *et al.* 2010). However, subsequent mutagenesis analysis showed that, while it is indispensable for the assembly and stability of Complex-I, this HL helix is unlikely to be actively involved in transmitting energy from the Q-site to the pumps (Belevich *et al.* 2011; Steimle *et al.* 2015; Zhu and Vik 2015). Furthermore, homologous elongated membrane arms are also found to couple with a variety of electron-input modules other than the NADH-quinone redox arm (Schuller *et al.* 2019; Yu *et al.* 2018), strongly supporting the notion that a common mechanism of proton translocation exists in all membrane arms of this group of redox-driven proton pumps (Efremov and Sazanov 2012). Next, we will discuss the energetic aspects of this common mechanism.

ENERGY COUPLING IN COMPLEX-I

In each functional cycle of Complex-I, four protons are extracted from the cytoplasm and expulsed to the periplasmic space through the membrane arm (Verkhovskaya and Bloch 2013). During this process, protons move towards the membrane side of higher electrochemical potential, and such movement requires driving energy. This energy is supplied through reduction of quinone, in the process of which two electrons are accepted from the buffer zone located in the redox arm. It has been suggested that most of the energy from NADH oxidation is released at the Q-model to generate a single power stroke, upon delivery of both electrons to quinone (Verkhovskaya *et al.* 2008); we refer to this process as injection of an electron pair. While the "external" redox energy propagates from the Q-module towards the distal end of the membrane arm, the energy flux decreases across each successive interface between neighboring pumps (Fig. 2A).

The quinone reduction can be divided into steps of Q-binding, electron injection (*i.e.,* formation of Q^{2-}), neutralization by Q^{2-}-protonation, and release of the redox product—quinol (QH_2) (Efremov and Sazanov 2012). Interruption of any of these steps halts the Q-reduction cycle. According to an updated view of the process (Kaila 2018), the neutralization step can be further divided into protonation of Q^{2-} by local titratable amino acid residues and subsequent regeneration of these proton donors. Nevertheless, the scheme of charge alternation remains the same, and we will stick to the first description for simplicity. While the presence of intermediate semiquinone species may render this process more complex, certain sub-steps can be referred to as one single step, at least for the purpose of discussing the thermodynamic mechanisms involved. Each of the steps during reduction of quinone releases mechanical (conformational) and/or electrostatic energy, and importantly the sum of these energy terms equals the redox energy of quinone in "solution" (*i.e.,* in the absence of the enzyme). Thus, both the partition of the total energy into multiple steps and the time sequence of release of the partitioned energy are of fundamental importance to our understanding of the proton-pumping mechanism of Complex-I. However, little is currently known about the detailed processes responsible for the energy partition. For instance, formation of the Q-binding site is dynamic (Babot *et al.* 2014; Galkin *et al.* 2008; Zhu *et al.* 2016), and is induced by the quinone binding with an "induced-fit" mechanism. Therefore, it is likely that quinone binding to the Q-site is directly coupled to the putative conformational transition of the P_P-module required for proton pumping (Kaila 2018). Furthermore, it is widely assumed that the dynamic formation of the Q-binding site generates a power stroke which drives the proton translocation. In a recent report (Cabrera-Orefice *et al.* 2018), it was shown that by immobilizing a loop inside the Q-binding pocket, the Q-reduction becomes decoupled from proton pumping, suggesting that a conformational change of this key loop generates the power stroke that drives all four pumps in the membrane arm. By restricting the movement of the key loop, it appears possible that a kinetically more favorable reaction path forms for the Q-reduction, and thus proton pumping becomes unnecessary. However, how exactly the power stroke propagates along the membrane arm remains to be elucidated.

Because no prosthetic group is embedded in the membrane arm, a direct (redox-driven) energy-coupling

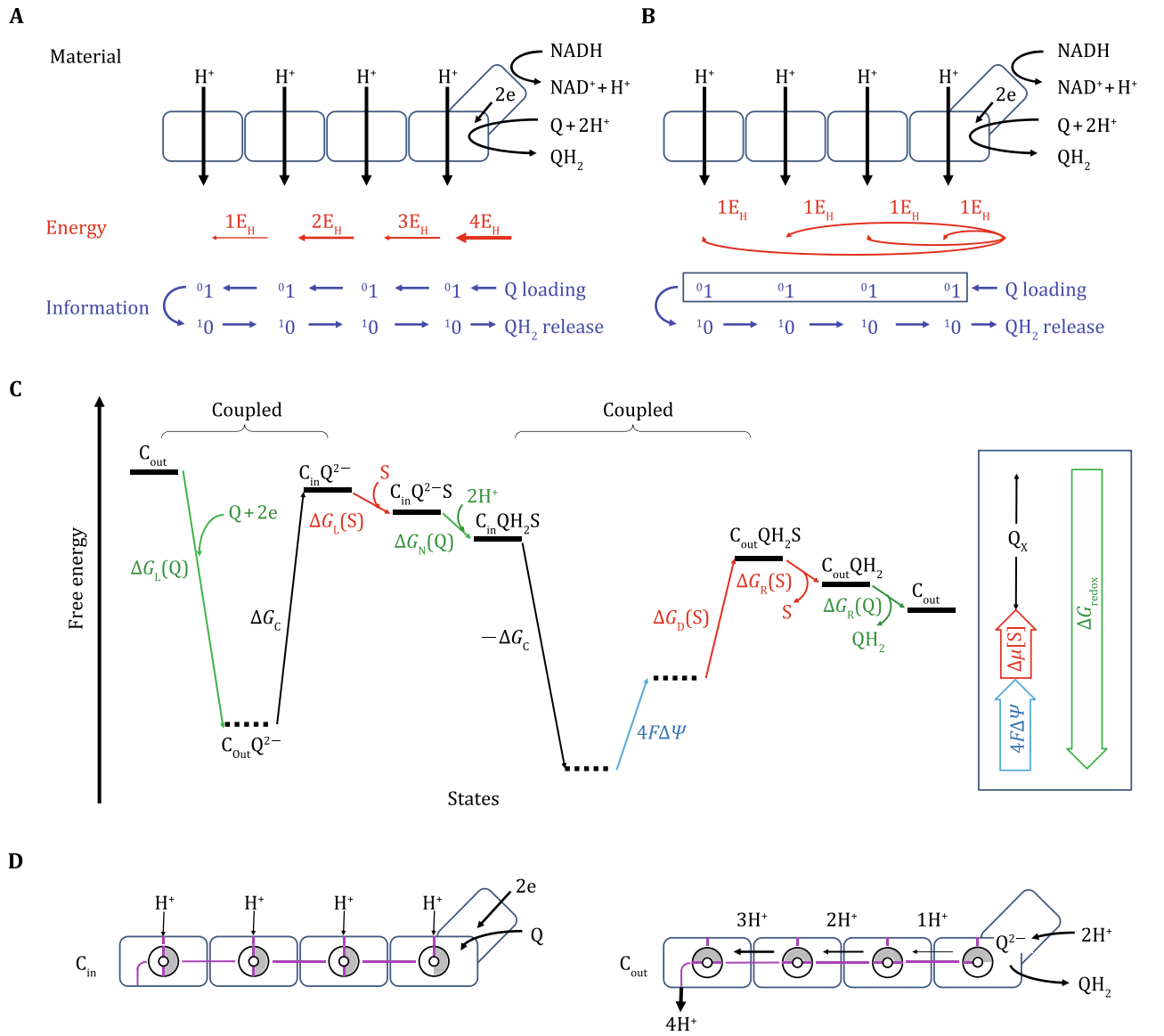

Fig. 2 Flows of material, energy, and information in Complex-I. **A** Canonical view of the energy propagation along the membrane arm. **B** An alternative view of the energy propagation. The energy required to transport one proton is denoted as E_H. The outward-facing conformation (C_{out}) is referred to as state 0; and the inward-facing conformation (C_{in}) as state 1. Thus, the C_{out}-to-C_{in} transition is denoted as ^{0}1; and the C_{in}-to-C_{out} transition as ^{1}0. **C** Simplified landscape of the free energy of the proton pumps. A Gibbs-energy landscape plot describes the thermodynamic relationship between different states. Horizontal lines represent states. Downward and upward thin arrows represent exoergic and endoergic transitions between states, respectively. *Green arrows* are associated with the energy of Q-reduction. *Red* and *cyan arrows* are associated with the chemical and electrostatic potentials of the substrates, respectively. Subscripts "L" and "R" refer to energy terms associated with loading and releasing, respectively. Collectively, the steps shown in this plot must meet the requirements of the First and Second Laws of thermodynamics. The starting and ending states are identical (*e.g.,* C_{out} is chosen arbitrarily), only being differed by the energy dissipation (*i.e.,* Q_X) of all four pumps during one functional cycle of Complex-I. Notes: (1) Many energy terms in the plot are variable, depending on the cellular/experimental conditions, *e.g.,* the membrane potential $\Delta\Psi$ and ΔpH. (2) Steps marked as "coupled" are likely to occur simultaneously. **D** Hypothetical antiporter-type pumping mechanism of Complex-I. Schematic diagram of the proton-pumping mechanism of Complex-I is shown. The conformational switch in each proton pump is depicted as a half-shaded ring. Potential proton wires are depicted as magenta lines

mechanism similar to those found in Complexes-III and IV can be ruled out. Instead, all four proton pumps in Complex-I are likely to function via indirect (conformation-driven) coupling of electron injection with proton pumping (Sazanov 2015). Intriguingly, in the hydrogen gas-evolving membrane-bound

hydrogenase (MBH) complex—a homolog of Complex-I, the electron-acceptor subunit, MbhM, is only loosely associated with the pump module (Yu *et al.* 2018), rendering tight mechanical energy transmission through precise, cooperative, inter-subunit conformational changes unlikely. In contrast to mechanical interactions, both electron injection and neutralization directly alter the electrostatic field inside the membrane arm. Thus, in principle, these two events have the potential to drive cycles of conformational changes of the antiporter-like subunits through long-range electrostatic interactions. A similar principle of electron-driven conformational changes in proton pumps of Complex-I has been postulated before (Efremov and Sazanov 2012), albeit without detailed discussion on the possible mechanisms behind the proposed long-range coupling between the Q-module and the proton pumps.

While an energetically balanced "resting state" structure is defined by a set of existing interactions, electrostatic interactions are additive in nature. Therefore, excitation of the resting state by an "extra" electric charge (such as injection of an electron pair) can be treated as independent of other preexisting interactions, simplifying our analysis on the energy converting process. Previously, we proposed that the interaction between the electrostatic membrane potential ($\Delta\Psi$) and a charged ligand can drive the conformational transition essential for functions of membrane proteins (Zhang and Li 2019). In a PMF-driven secondary active transporter, for example, the electrostatic force exerted on a proton immersed in the electric field of $\Delta\Psi$ ($\sim$100 mV, corresponding to an electric charge density of $\sim$0.02 e_0 per 1000 Å^2) is typically $\sim$5 pN (Zhang *et al.* 2015). In comparison, the injection of two "extra" electrons generates an electrostatic force on a unitary charge (*e.g.,* a proton):

$$F \equiv \frac{2e_0^2}{(4\pi r^2 \varepsilon \varepsilon_0)} \approx 5 \times 10^4/(\varepsilon \cdot r^2)(\mathrm{pN}),$$

where the distance (r) is measured in Å unit. Assuming a dielectric constant (ε) of two in the membrane arm, a force (F) of approximately 2.5 pN is generated at a 100-Å distance. Such a force is exerted on each and every electric charge in the membrane arm. With proper distribution of electric charges in the proton-pumping subunits, the combined electrostatic forces and associated mechanical torques are presumably sufficient to drive the conformational changes required for proton transport. Importantly, it is the overall force and rotational torque generated by combination of electric forces, structure constrains from the neighboring domains, as well as the hydrophobic interactions with lipid bilayer (*e.g.,* via the amphipathic structural elements) that determine the conformational change of a given domain within the membrane arm. For instance, the positive-inside and negative-outside charge distribution in each domain of the antiporter-like subunits and its associated overall electric dipole potentially contribute to the electrostatic interactions required for the conformational changes of the proton-pumping subunits. Moreover, two types of interactions have been described for $\Delta\Psi$-driven conformational changes of membrane proteins (Zhang and Li 2019). The first type of conformational change is caused by changes in electric charges of the protein, under the condition of constant external $\Delta\Psi$, as exemplified by the electrogenic secondary active transporters (Zhang *et al.* 2018a). The second type is caused by a change of external $\Delta\Psi$, with the electrostatic charges (*e.g.*, of basic residues) permanently attached to the protein structure, as exemplified by the voltage sensors in voltage-gated ion channels (Zhang *et al.* 2018b). In Complex-I, the electrostatic interactions between the injected electron pair and the antiporter-like subunit *per se* (*i.e.*, in the absence of the substrate proton) are more similar to the second type. In particular, the "external" electrostatic field changes abruptly upon electron injection, whereas the electrostatic charges are kept fixed with mobile structural elements of the proton pumps. Next, we will discuss the properties of these mobile structural elements.

GENERAL MECHANISM OF PROTON PUMPS

According to the now well-established general "alternating-access" mechanism of transporters (Jardetzky 1966), each proton pump must possess (at least) two major conformations, namely the inward- and outward-facing conformations, or C_{in} and C_{out}. For those so-called peristaltic pumps, the two major conformations are referred to the terminal states in which the substrates are loaded and released. The conformational change associated with substrate transport may be considerably large, as exemplified by the transport cycle of MFS transporters (Abramson *et al.* 2003; Dang *et al.* 2010; Huang *et al.* 2003), or more subtle as exemplified by the light-driven proton pump of bacteriorhodopsin (Wickstrand *et al.* 2015) [but also see Weinert *et al.* (2019)]. Importantly, the structurally observed ground state of Complex-I seems to connect the central proton-binding site to the periplasmic space (Sazanov 2015) (also see below), thus likely representing the C_{out} state. It is conceivable that, beside this ground state, the proton-pumping subunit possesses an excited state that connects the central proton-binding site to the cytoplasmic side of the membrane. On the basis of their

analogy with general transporters, we propose that the proton-pumping subunits in Complex-I follow the same alternating-access mechanism as found in general transporters. In support of our hypothesis, it is well established that the deactive form of *Bos taurus* Complex-I functions as an antiporter, catalyzing electroneutral Na^+/H^+ exchange across the inner mitochondrial membrane (Roberts and Hirst 2012). Because of currently limited structural information on conformational changes in the membrane arm of Complex-I, we focus here on antiporter-like subunits located in the P_D-module, without discussing the mechanistic details of the P_P-module. It should be noted that our model ascribes the two major conformations, C_{in} and C_{out}, to the proton-pumping subunits, not to the active and deactive conformations of the overall Complex-I. The conformational changes in the antiporter-like subunits are of a rate of 10^4-cycles per min (Vinogradov 1998), whereas the rate of Complex-I activation occurring in the Q-module is in the range of 1–10 events per min (Kotlyar *et al.* 1992). Moreover, in order to drive subsequent proton translocation, the C_{in} is likely to represent a state of sufficiently high conformational energy compared to the ground C_{out} state. Therefore, a major challenge in studying the structural changes on Complex-I lies in identifying the C_{in} and C_{out} states of the proton pumps as well as their associated half-channels for the translocation of substrate protons.

The conformational transition in the proton pump could be driven by either mechanical forces or electrostatic forces. While mechanical forces are short-range interactions depending on fairly rigid structural elements, electrostatic forces can be long-range interactions if mediated by low-dielectric material. Currently, it is not clear how the redox energy from Q-reduction is partitioned between mechanical and electrostatic forms. As shown in Fig. 2A, it can be envisioned that the external energy from the Q-redox reaction first triggers the C_{out}-to-C_{in} conformational transition in the proton pump of the P_P-module. In turn, other pumps (NuoN, M, and L) in the P_D-module are sequentially converted from the C_{out} state to the C_{in} state. Once the distal pump (NuoL) is driven into its C_{in} state, loading of the substrate proton triggers the C_{in}-to-C_{out} conformational transition. Subsequently, the proton is released in the C_{out} state. In turn, other pumps switch back to the C_{out} state in a domino manner. Once protons are released from all four pumps, the redox product QH_2 is released from the Q-module, and the system proceeds into the next cycle (Sazanov 2015). Because it would require many precise short-range mechanical interactions along the membrane arm, we disfavor such a model. An alternative excitation mechanism of proton pumps in Complex-I is the wave-spring mechanism, which was previously proposed to explain the process of conformational transition based on the electrostatic interactions (Kaila 2018; Torres-Bacete *et al.* 2007). It states that the electron transfer signal propagates in a form of alternating protonation, from the Q-module to the distal end and then bounces back. However, such a mechanism was criticized because it would also require a very precise design to achieve proton gating, which seems incompatible with the inherent protein flexibility in Complex-I (Sazanov 2015).

Here, we postulate that the redox-energy transmission simultaneously occurs in the form of long-range electrostatic interactions in all four pumps inside the membrane arm, as shown in Fig. 2B. In other words, transitions from the ground (C_{out}) state to the excited (C_{in}) state in the four pumps are not necessarily sequential. Interestingly, the HL helix seems to play a critical role in such electrostatic excitation. Without the clamping effect on the three antiporter-like subunits exerted by the HL helix, the long membrane arm might be torn apart by the electrostatic power strokes, which originate from the electron injection and must be sufficiently powerful to drive proton transport in all four pumps. Next, we put forward the argument that proton pumps in Complex-I behave similarly to a specific well-described transporter category, namely antiporters.

ANTIPORTER-TYPE MECHANISM

The communication between the substrate and driving substance is of critical importance in the mechanisms of any active transporter. For example, secondary active transporters can be classified into symporters and antiporters. By definition, in the case of a symporter, binding of both the substrate and driving substance (*e.g.,* H^+ or Na^+) to the transporter must be cooperative; in contrast, for an antiporter, binding of the substrate and driving substance to the transporter must be competitive (Zhang *et al.* 2015). More specifically, in a symport process, the substrate usually binds to the ground state first and thus facilitates binding of the driving substance by manipulating the micro-environment to increase the affinity of the driving substance. In turn, binding of the driving substance immediately exerts a force to drive the transporter into its excited state. (The opposite order of bindings would require an unlikely mechanism, in which binding of the driving substance creates a large transitional energy barrier subsequently reduced by binding of the substrate.) In the excited state, the substrate and the driven substance are released sequentially; the transporter subsequently

returns back to its low-energy ground state. In an antiport process, in contrast, the driving substance usually binds to the ground state first, and consequently drives the transporter into its excited state. Subsequently, the substrate binding induces the release of the driving substance, and the energy stored in conformational change pulls the transporter back to its ground state, being accompanied with substrate transport. No matter which of the two mechanisms is used, binding and release of the driving substance appear to be the two most critical events in the functional cycle of an active transporter. In any active transporter, it is the energy released by the driving substance during conformational change of the transporter rather than the substance *per se* that drives the conformational changes. For example, in the absence of PMF, binding of a proton is unlikely to continuously drive a transporter. Therefore, structural biology studies on secondary active transporters should aim to investigate the detailed mechanisms of either cooperativity or competition between the substrate and driving substance (Zhang *et al.* 2015, 2018a).

In the context of this paper, we wondered whether the same principle responsible for the function of driving substances is applicable to Complex-I as a redox-driven primary active transporter. It is well established that in a secondary active transporter, the substrate and driving substance usually share the same transport path. In contrast, in a redox-driven transporter, the driving substance (*i.e.,* the injected electron pair) does not utilize the transport path of the substrate (protons). While this fundamental difference exists, electron injection and neutralization can still be considered the two key events responsible for the conformational transitions of proton pumps in Complex-I. One may hypothesize two possible yet mutually exclusive schemes. First, assuming that C_{in} represents the ground state, the substrate protons could bind to the pumps from the cytoplasm; only afterwards, the electron injection occurs, driving the C_{in}-to-C_{out} transition. Subsequently, the substrate protons are released, followed by neutralization of electron pair as well as the C_{out}-to-C_{in} transition. Such scenario would represent a symporter-type mechanism. Second, assuming that C_{out} represents the ground state, formation of Q^{2-} drives the C_{out}-to-C_{in} transition and maintains the excited C_{in} state, in which the pump waits for the loading of substrate protons. The complete loading of substrates triggers the neutralization of the electron pair by Q^{2-} protonation, withdrawing the electrostatic forces that maintain the high-energy C_{in} state. Consequently, the pumps return to their ground C_{out} state, carrying their substrate protons to the periplasmic side. In turn, release of all substrate protons triggers release of the redox product QH_2, and the transporter proceeds into the next function cycle. Such scenario would represent an antiporter-type mechanism.

As all currently available crystal structures of Complexes-I were determined in the absence of injected electrons, presumably representing the ground (C_{out}) state, we believe that the antiporter-type coupling scheme is a more likely mechanism responsible for conformational transitions in proton pumps of Complex-I. A similar principle coupling electron transfer and conformational transition in Complex-I was discussed before, albeit based on a two-stroke two-pump model (Brandt 2011) which remains controversial (Efremov and Sazanov 2012; Parey *et al.* 2018).

A simplified energy landscape of the proton pumps in Complex-I, which utilizes the antiporter-type mechanism, is provided in Fig. 2C. The change of the chemical potential of the substrate (S, *i.e.,* four protons), $\Delta\mu(S) \equiv 4 \times 2.3RT\Delta pH$, can be divided into three interdependent terms: $\Delta G_L(S) \equiv 9.2RT(pH_{in} - pK_{a,in})$, the proton loading energy; $\Delta G_D(S) \equiv 9.2RT\ (pK_{a,in} - pK_{a,out})$, denoted as the differential binding energy and likely being a large positive term; and $\Delta G_R(S) \equiv 9.2RT\ (pK_{a,out} - pH_{out})$, the proton releasing energy. Similarly, the Q-reduction energy, ΔG_{redox}, can be divided into three parts: $\Delta G_L(Q)$ for Q-loading plus electron injection; $\Delta G_N(Q)$ for neutralization by Q^{2-}-protonation; and $\Delta G_R(Q)$ for QH_2 release. Here, $\Delta G_L(Q)$ is hypothesized to be the major step of energy input, and is converted to conformational energy, ΔG_C, via the electrostatic interactions described above. Loading of substrates and neutralization of electrons results in release of ΔG_C, driving the subsequent C_{in}-to-C_{out} transition while simultaneously compensating for the electrostatic energy $4F\Delta\Psi$ (where "F" stands for the Faraday constant) as well as the differential binding energy, $\Delta G_D(S)$, which is equivalent to a Nernst-like voltage $V_D \equiv \Delta G_D(S)/4F \approx 59\ mV(pK_{a,in} - pK_{a,out})$. The box on the right side of Fig. 2C contains two primary terms: (1) the external energy input, ΔG_{redox}, originating from the quinone reduction; and (2) the total energetic gain of all protons including both $\Delta\mu(S)$ and $4F\Delta\Psi$. Ratio of these two primary terms represents the efficiency of the energy conversion by Complex-I; and the difference between them is defined as Q_X (≥ 0, where the subscript "X" stands for the so-called thermodynamic force in chemical kinetics (Hill 1989)). On the one hand, if releasing of the driving energy is coupled properly with the progress of the functional cycle of proton pumps, Q_X is positively correlated with the overall rate of the transport. More specifically, $Q_X = RT\ln(J_+/J_-)$, where "J_+" and "J_-" represent the positive and negative fluxes,

respectively, of the reaction. On the other hand, Q_X is negatively related to the efficiency of energy conversion. Consequently, the overall rate is negatively related to the efficiency. With these energetic concepts in mind, we will move forward to discuss structural basis of conformational change in the proton pumps in Complex-I.

STRUCTURAL BASIS OF THE TWO-STATE TRANSITION

Most 3D structures of transporters possess a certain pseudosymmetry (most commonly twofold symmetry), often originated from gene duplication (Pornillos and Chang 2006; Shi 2013; Zhang *et al.* 2018a). This type of internal structural symmetry implies that the C_{in} and C_{out} states are also symmetrical, in agreement with the symmetry of the lipid bilayer and probably reflecting the evolution history of most transporters. Translocation pathways for substrates are often located in the symmetrical interface between structural repeats. Importantly, the structures of the antiporter-like subunits in the membrane arm of Complex-I appear to obey the same principle, albeit with a twist.

In addition to being homologous in their primary sequences, the three Mrp antiporter-like subunits (NuoL, M, and N) share similar overall folding patterns (Efremov and Sazanov 2011). Each subunit contains 14 conserved transmembrane helices (TMs 1–14), forming two domains namely the N_{TM} domain (containing TMs 1–8) and C_{TM} (TMs 9–14) (Fig. 3A). In each subunit, the β-hairpin of the βH-belt is located between TMs 2 and 3 of the N_{TM} domain, and the α-helix of the βH-belt is attached to the C-terminus of TM14 of the C_{TM} domain. Usually, the presence of such amphipathic structural elements implies that their associated TM helices undergo large conformational changes during the functional cycle of the host integral membrane protein (Zhang and Li 2019). Moreover, the distal NuoL subunit contains two extra TM helices. The HL helix is stretched between TM15 and TM16 of NuoL, and mainly contacts the C_{TM} of each Mrp antiporter-like subunit.

More importantly, TMs 4–8 of N_{TM} and TMs 9–13 of C_{TM}, each forming a 5-TM helix bundle, are related by a pseudo twofold screw symmetry (*i.e.,* a 180° rotation plus a translation along the rotation axis which is parallel to the membrane plane), also called inversion symmetry (Fig. 3B). In addition, the C_{TM} of one subunit and the N_{TM} of its distal-side neighboring subunit are also related by a similar, pseudo twofold screw symmetry. Therefore, the three antiporter-like subunits form a string of six 5-TM repeats in a head-to-tail manner. Moreover, both TM7 and TM12 (*i.e.,* the 4th helix in each 5-TM repeat) contain a break as well as an inserted short loop in the middle, resulting in the formation of helix segments TM7a, TM7b, TM12a, and TM12b. These two helix breaks are signature features of the Mrp antiporter-like subunits (Baradaran *et al.* 2013; Schuller *et al.* 2019; Yu *et al.* 2018; Zhu *et al.* 2016; Zickermann *et al.* 2015). Similar helix breaks are often found to form ion-binding sites in the middle of integral membrane proteins (Screpanti and Hunte 2007). In addition, TM8 contains a conserved π-bulge in the middle, presumably by the insertion of a single residue (*e.g.,* Ala255 in *E. coli* NuoL) compared to a standard α-helix (*e.g.,* TM13). Because it remains energetically unfavorable during protein folding (Cooley *et al.* 2010), this π-bulge within TM8 strongly implies an important yet unknown functional role. In the string of 5-TM repeats, however, a twofold symmetrical interface that might serve as a potential translocation pathway for the substrate (similar to those found in MFS transporters) is lacking.

More detailed analyses of experimentally determined, ground-state structures of Complexes-I consistently show that the intra-subunit packing pattern between 5-TM helix bundles of N_{TM} and C_{TM} is distinctively different from that of the inter-subunit packing (Fig. 3A, B). This deviation from repeating of true twofold screw symmetry becomes clearer near the breaks of TM7 and TM12. In particular, the break region of TM7 in N_{TM} contacts both TMs 9 and 10 (*i.e.,* the 1st and 2nd helices of the 5-TM helix bundle) in C_{TM}, whereas the break region of TM12 in C_{TM} contacts only TM5 (*i.e.,* the 2nd helix of the 5-TM helix bundle) from N_{TM} of the neighboring subunit. Importantly, in each subunit, the cytoplasmic half of the intra-subunit N_{TM}–C_{TM} interface is highly hydrophilic, suggesting a potential half-channel towards the cytoplasmic side for substrate protons (Baradaran *et al.* 2013). Nevertheless, this interface is essentially closed in the crystal structure, necessitating a conformational change for the half-channel to open. Because of the deviation from repeating of true twofold screw symmetry, the three antiporter-like subunits in the membrane arm form a curvature within the plane of the membrane (Efremov *et al.* 2010), instead of being aligned in a straight line. The concaved side of the curve is maintained by the pulling force exerted by the HL helix near the cytoplasmic surface of the membrane. In contrast, the convex side of the curve is maintained by the pushing force exerted by the βH-belt near the periplasmic surface of the membrane. As mentioned above, the HL helix contacts more solidly with the C_{TM} domain from each of the three antiporter-like subunits than with the N_{TM} domain (Efremov *et al.* 2010),

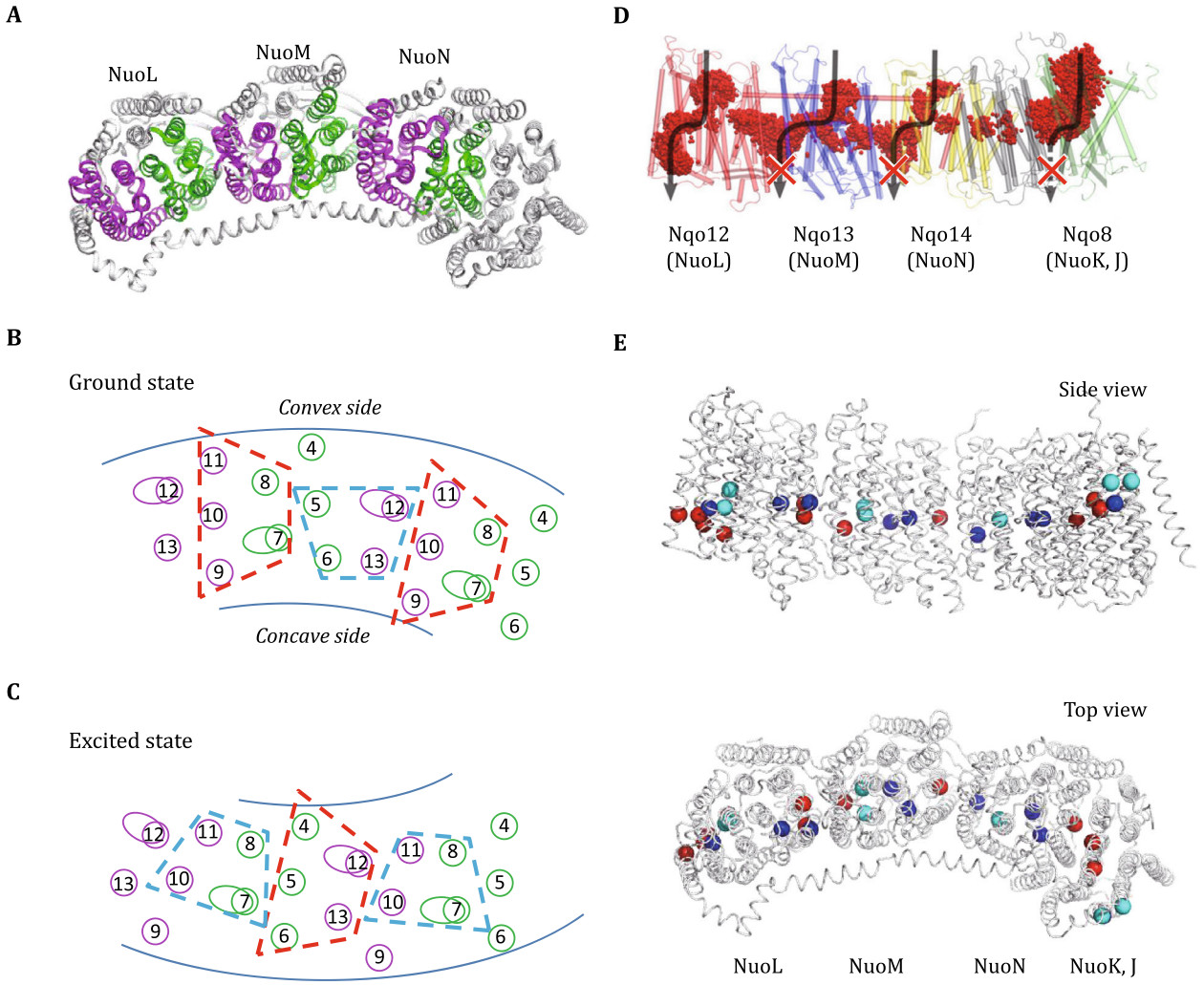

Fig. 3 Putative conformational change and central polar axis in Complex-I. **A** Top (cytoplasmic) view of the membrane arm of *E. coli* Complex-I (PDB ID: 3RKO). The 5-TM helix bundles in N_{TM} and C_{TM} domains are indicated in *green* and *magenta*, respectively. **B** Packing of the 5-TM bundles from two neighboring antiporter-like subunits in the ground state. Each TM helix is represented by a cycle, and the breaks present in TM7 and TM12 are depicted as ovals. Two types of inter-domain packings are marked with *red* and *cyan* trapezoids. **C** Alternative packing of the 5-TM bundles in a putative excited state. **D** Water clusters as potential proton paths. Water molecules accumulated during the MD simulation are depicted as *red spheres*, and previously proposed proton paths as *gray arrows*. This panel was adopted from Di Luca *et al.* (2017). **E** The central polar axis identified in the crystal structure of *E. coli* Complex-I (PDB ID: 3RKO). Positions of the Cα atoms of acidic (Asp and Glu), basic (Lys and Arg), and His residues are shown as *red*, *blue*, and *cyan spheres*

allowing a higher degree of freedom for the latter to rearrange its packing.

This observed difference between the two types of inter-domain packing suggests a possibility that alternating between them is associated with a dramatic conformational change (Fig. 3C). In particular, if the N_{TM} and C_{TM} domains systematically switch their packing pattern from the observed ground state to the alternative state, the curvature of the membrane arm will be reduced and possibly even become inversed. Such conformational change requires a rotation ($\sim 20°$ about an axis approximately perpendicular to the membrane plane) of the N_{TM} domain relative to its neighboring C_{TM} domains. We hypothesize that such N_{TM}–C_{TM} repacking is associated with the C_{in}–C_{out} transitions of the antiporter-like subunit, thus switching the connection of the central substrate-binding site featuring distinct half-channels. Clearly, the breaks in TM7 and TM12 are essential in defining the inter-domain repacking. Interestingly, the conserved π-bulge in the middle of TM8 seems to stabilize both the C_{out} and C_{in} states by alternating its packing with TM11, thus functioning as a toggle switch. Because of the restrictions from both the HL helix and βH-belt, our proposed conformational change requires an external energy input, presumably from the electrostatic forces of the electron injection. In

particular, the relative rotation between N_{TM} and C_{TM} requires distinct mechanical torques to drive. Consequently, the input energy is (partially) stored in the form of conformational stress (ΔG_C in Fig. 2C). According to our antiporter-type mechanism, the energy of this conformational stress will be release to drive substrate transport upon electric neutralization at the Q-module. Furthermore, it is well established that the mature mitochondrial Complex-I forms a respiratory-chain supercomplex (*i.e.*, respirasome) by exclusively associating with respiratory Complexes-III and -IV (Formosa *et al.* 2018). Our proposed conformational transitions in the membrane arm of Complex-I appear not to interfere with the formation of this respirasome (Dudkina *et al.* 2011).

According to the Boltzmann distribution, in the absence of input energy the excited-state conformation of a single pump subunit has a low population (<2%), because of its high energy level (>4*RT*) required to drive translocation of each proton across the (~100 mV) $\Delta\Psi$ with additional ΔpH. Therefore, such an excited-state conformation is difficult to be captured in structural studies, unless it is stabilized by a "lucky" mutation or by inhibitor binding. Certain Complex-I inhibitors may bind to a specific conformation of the antiporter-like subunit, preventing conformational transitions and thus stopping the functional cycle of Complex-I. In fact, fenpyroximate is a potent inhibitor of Complex-I, and its photo-labeling derivative was found to specifically bind to the distal ND5 subunit (a homolog of NuoL) in *B. taurus* mitochondrial Complex-I. The labeling is enhanced by NADH, but is diminished by inhibitors that are known to bind to the Q-module presumably locking Complex-I in its ground state (Nakamaru-Ogiso *et al.* 2003). These observations are consistent with our hypothesis of domain repacking if it is assumed that fenpyroximate preferentially binds to the excited state of NuoL. In addition, results from a Cys-based cross-linking experiment suggest that mobility of TM5 of NuoM relative to TM13 of NuoN is essential for the proton-pumping activity of Complex-I (Zhu and Vik 2015). A conceptually similar two-state conformational change was explored before in a study using molecular dynamics (MD) simulation (Kaila *et al.* 2014). However, the molecular models used in that simulation study focused only on subtler conformational changes of TM7 and TM8. In comparison, our model is likely to be more consistent with the differential cross-linking data obtained for Complex-I both in NADH-bound and NADH-free form, which suggest large conformational changes in the interfaces between antiporter-like subunits during their functional cycles (Zhu and Vik 2015). Taken together, we propose our model of N_{TM}–C_{TM} repacking in the antiporter-like subunits based on the following reasoning: (1) A large conformational change that is able to store sufficient energy to drive the energy-consuming proton transport seems necessary; (2) Conservation of the intrinsic symmetry in the Mrp-like antiporters is most likely to be relevant to the pumping process; (3) Several highly conserved structural features (*e.g.,* the π-bulge in TM8) are likely to be functionally required. To further explore the mechanism of the antiporter-like subunits, we will next discuss the relationship between these large conformational changes and formation/deformation of proton paths.

POTENTIAL PROTON WIRES

Electron transfer between biological molecules often occurs via a quantum tunneling mechanism, provided that donor–acceptor distance (tunneling length) is less than 15 Å. In contrast, however, proton translocation can only occur via hand-to-hand delivery through proton wires embedded in the proton pumps (Wraight 2006). The underlying explanation for this phenomenon is the fact that the tunneling length is proportional to $(\text{mass})^{-1/2}$. As protons are over 1800-fold heavier than electrons, their tunneling length is much shorter. According to the alternating-access model of general transporters, a proton pump should possess two half-channels alternating in their connection to the central proton-binding site. Detailed structural analysis of Complex-I suggests that the C-terminal halves of the broken helices TM7 and TM12 (*i.e.,* TM7b and TM12b) are involved in the formation of the half-channels for substrate protons (Efremov and Sazanov 2011). In addition, MD simulations show that water molecules are dynamically distributed inside the membrane arm of Complex-I (Di Luca *et al.* 2017) (Fig. 3D). These water molecules only populate the neighborhood of polar residues, suggesting potential paths for proton translocation (*i.e.,* proton wires). More specifically, water molecules form two major clusters in each antiporter-like subunit, namely in the cytoplasmic half of the N_{TM}–C_{TM} interface and within the periplasmic half of the C_{TM} domain. On the basis of these observations, it can be hypothesized that these two water clusters form parts of the inward and outward half-channels. Importantly, the cytoplasmic-side water cluster is likely to become fully connected with the bulk cytoplasm upon repacking of the N_{TM}–C_{TM} interface and transition to the C_{in} state. It should be emphasized that the two half-channels are not allowed to connect with each other to form a full channel. Otherwise, the transmembrane electrochemical potential of protons would be dissipated via the

transient full channel. Therefore, the conformational change occurring inside the pump subunit results in switching connection of the central proton-binding site between the two distinct half-channels, not however in bridging the two channels. For example, upon transition to the C_{in} state, the central proton-binding site appears to disconnect from the water cluster in the C_{TM} domain by blocking the path with the sidechains of a few hydrophobic residues (*e.g.,* the highly conserved Leu239 of NuoL and Leu244 of NuoM in *E. coli*) from the N-terminus of TM7b. In addition, the connectivity of central polar axis is likely to change upon the domain repacking. As will be discussed below, this structural change in the central polar axis is likely to affect the formation of the exit half-channel, thus providing an additional mechanism to implement the C_{out}–C_{in} transition.

Certain high-density water clusters shown in the MD simulation may represent buffer zones for the substrate protons. They will become part of the proton wire only when being fully connected to the exo-membrane space. In fact, among the C_{TM} water clusters, only the one in the distal subunit (NuoL) is clearly connected with the periplasmic space. In contrast, the other two clusters (in NuoM and N) appear to be blocked by substantial hydrophobic residues, and are thus unable to directly connect with the periplasmic side in the crystal structures (Sazanov 2015). As the state transition in our proposed dynamic model is unable to induce a conformational change within the C_{TM} domain, these two water clusters inside the C_{TM} domains of NuoM and N are unlikely to become directly connected with the periplasmic side in the excited state either. Another MD simulation study of Complex-I also suggests that its central polar axis is extensively connected via water networks to the cytoplasm, not however, to the periplasm except in the distal NuoL subunit (see Fig. 4 in Kaila *et al.* (2014)). Therefore, the proton paths shown in Fig. 3D previously proposed in Di Luca *et al.* (2017) are likely to be only partially reflecting reality. A possible solution to this "chocking" problem should surface once our model is further refined (see below).

CHANGE OF THE PK_A VALUE OF THE PROTON-BINDING SITE

Although the exact identity of the proton-binding site in each antiporter-like subunit remains elusive, several conserved protonatible residues near the break of TM7 represent suitable candidates. It is also possible that a few such groups together organize a buffer zone acting as a proton trap. For a pump to effectively transport protons against a pH gradient across the membrane, the pK_a (*i.e.,* proton-binding ability) of the central proton-binding site is likely to assume a fairly high value in the loading state and to switch to a rather low value in the releasing state. On the one hand, in a given antiporter-like subunit, such a difference in its affinity to the substrate protons favors both proton loading in the C_{in} state and proton release in the C_{out} state, and it raises the chemical potential of the substrate protons upon the C_{in}-to-C_{out} transition. On the other hand, this difference in affinity between C_{in} and C_{out} is associated with a positive ΔG_D. Since it has to be compensated by the external energy input, the amplitude of ΔG_D should not exceed this input (Fig. 2C).

In each antiporter-like subunit, the cytoplasmic side (*i.e.,* N-terminus) of TM10 contains two strictly conserved basic residues, *e.g.,* Lys305 and Arg306 in *E. coli* NuoL. They are likely to assume distinct effects on the central proton-binding site in the C_{in} and C_{out} states. In our predicted C_{in} state, the N_{TM}–C_{TM} interface opens, forming a solvent accessible crevice or half-channel. In this case, the high dielectric permittivity of solvent weakens the electrostatic effect of the conserved basic residues on the proton-binding site. In contrast, in the ground C_{out} state, the crevice is closed, and solvent is removed from the interface. Consequently, the basic residues will exert a stronger positive electrostatic field on the proton-binding site, drastically reducing its pK_a value. Similar pK_a-adjusting mechanism has been proposed for the positively charged motif-B in certain PMF-driven MFS transporters (Heng *et al.* 2015). It is important to note that the pK_a value of the central proton-binding site critically depends on the substrate-binding status, thus strongly affected by the connectivity to other parts of the proton transport network, which will be discussed next.

THE CENTRAL POLAR AXIS

According to our model, injection of the electron pair to the bound quinone is most likely to occur in the ground C_{out} state, but only after all substrate protons have been released from the pumps to the extracellular space. Otherwise, the C_{out}-to-C_{in} transition driven by the electron pair would carry the substrate protons back to the cytoplasm. Similarly, neutralization of the electrons by Q^{2-}-protonation most likely occurs in the C_{in} state, but only after the substrate protons have been fully loaded. Otherwise, the pumps would not carry sufficient numbers of protons during the ΔG_C-driven transition back to the ground state. In either of these (abnormal) cases, Complex-I would fail to efficiently convert the energy

from quinone reduction to proton pumping. Therefore, for Complex-I to function properly, it is essential that the pumps communicate effectively with the redox center.

As the redox reaction requires electron transfer, communication between the redox center and the pumps can be assumed to be of electrostatic nature. The electrostatic force in the elongated membrane arm of Complex-I more likely acts within and parallel to the membrane plane, albeit the apparent movement of the substrate protons occurs in a direction perpendicular to the membrane. Importantly, the conserved central polar axis extends through the entire arm (Baradaran *et al.* 2013) (Fig. 3E). It is generally agreed that this central polar axis plays an essential role in communicating across the membrane arm of Complex-I. However, the precise mechanism remains under debate. Based on our two-state model of the antiporter-like subunit, we propose a novel communication mechanism for the central polar axis, namely that upon C_{in}–C_{out} transition and N_{TM}–C_{TM} domain repacking, the central polar axis changes its internal connectivity and alternates its connection with the two sides of the membrane.

In the N_{TM} domain of each antiporter-like subunit, an ionic pair of Glu^{TM5}–Lys^{TM7} is highly conserved, forming part of the central polar axis. The charged sidechains of this ionic pair are more than 5 Å apart. As a consequence, they are unable to form a salt-bridge bond; instead, they form an electric dipole. In principle, such an electric dipole embedded inside the rigid N_{TM} domain is able to respond to the changes in the electric field associated with electron injection and neutralization, thus contributing to the rotation torque required to drive conformational transition of the N_{TM} domain relative to the remaining parts of the membrane arm. Nevertheless, if the only role of this ionic pair is to function as an electric dipole, a more hydrophobic micro-environment would be more beneficial. However, many of its surrounding residues are hydrophilic and are supplemented by additional water molecules. Furthermore, the Glu^{TM5}–Lys^{TM7} electric dipole present in NuoL is likely to be canceled by a nearby conserved dipole located in TM6, suggesting that the role of electric dipole is not conserved. Moreover, when they are well-aligned with the overall polar axis, for example in the crystal structures of the ground C_{out} state, these Glu^{TM5}–Lys^{TM7} ionic pairs are likely to participate in the formation of proton paths by contributing protonatible groups. In fact, functional studies using site-directed mutagenesis showed that these ionic pairs are extremely sensitive to mutation, whereas many other polar residues in antiporter-like subunits can be mutated without serious consequence (Amarneh and Vik 2003; Euro *et al.* 2008; Nakamaru-Ogiso *et al.* 2010; Torres-Bacete *et al.* 2007). For examples, $E144^{TM5}A/Q$ (but not $E144^{TM5}D$) in NuoM of *E. coli* Complex-I abolished the proton transport activity. Unexpectedly, in a small number of NuoN homologs, Glu^{TM5} is replaced by non-polar residues (see Fig. S8 in Efremov and Sazanov 2011), and mutational analysis showed that Glu^{TM5} in *E. coli* NuoN can be mutated to Ala/Cys/Asp with only minor effects on proton-pump activity (Amarneh and Vik 2003). However, in these cases, the loss of Glu^{TM5} may be compensated by adjacent acidic residues from the neighboring subunit NuoK, which seems to tightly bind with the N_{TM} domain of NuoN (Efremov and Sazanov 2011; Sazanov *et al.* 2000). Taken together, the most important role played by the conserved Glu^{TM5}–Lys^{TM7} ionic pair appears to be in the formation of a dynamic proton wire, whereas the contribution of Glu^{TM5}–Lys^{TM7} to the overall electric charge–dipole interaction reduces with its distance to the Q-module and varies from subunit to subunit.

In the NADH-quinone redox-driven Complex-I, the redox arm is located at the right side of the membrane arm (in the standard orientation shown in Fig. 1). In contrast, in the ferredoxin-proton redox-driven MBH complex, the redox arm is located on the left side of the membrane arm (Yu *et al.* 2018). This structural distinction may originate from their different redox reactions. In the Q-reduction catalyzed by Complex-I, the electron pair is first injected to the electroneutral quinone bound at the reaction center which is located on the negative side of the electric dipoles of the Glu^{TM5}–Lys^{TM7} pair; later, the electron pair is neutralized by Q^{2-}-protonation. In contrast, in MBH, it is more probable that electron acceptors, two protons, are first bound to the catalytic center which is located on the positive side of those electric dipoles; later, the protons are neutralized by the electron injection. In either case, the first-arrived substrate always promotes a clockwise rotation of the Glu^{TM5}–Lys^{TM7} pair as well as its host N_{TM} domain (viewed from the cytoplasmic side), probably resulting in the C_{out}-to-C_{in} transition. Therefore, our hypothetical model on the role of conserved central polar axis provides a possible explanation as to why the redox arm is located at opposite ends of the membrane arm in Complex-I and MBH.

MECHANISTIC MODEL OF THE PROTON PUMPS

Combining the results from the discussions above, we propose a mechanism of the proton pumps in Complex-I, depicted in Fig. 2D. Upon sequential binding of quinone and electrons to the redox center in the Q-module, all proton pumps are excited from the ground C_{out} state

into the C_{in} state, converting the electrostatic energy into the conformational energy (ΔG_C) stored in each proton-pumping subunit. As a first-order approximation, we only consider the primary, direct electrostatic interactions between the injected electron pair and electric charges of individual domains of the antiporter-like subunits, and ignore secondary effects arising from these primary events. This approximation appears reasonable, because the long-range electrostatic interactions between the Q-module and the proton pumps are instantaneous, whereas secondary effects will depend on subsequent, slower conformational changes as well as proton loading. In the excited C_{in} state, the central proton-binding site in each antiporter-like subunit is connected to the cytoplasmic side of the membrane, permitting substrate loading. Simultaneously, the proton wire along the central polar axis becomes broken into fragments because of the N_{TM} repacking with its neighboring C_{TM} domains on both proximal and distal sides. Based on discussion of the antiporter-type mechanism, we hypothesize that, upon the loading of substrate protons, a hitherto unidentified mechanism is responsible for triggering neutralization of the injected electron pair by Q^{2-}-protonation at the redox center. Upon withdrawing the electric forces, the stored ΔG_C in the C_{in} state is released. This released energy not only drives the C_{in}-to-C_{out} transition but also raises the electrochemical potential of the substrate protons (Fig. 2C). Subsequently, the proton wire along the central polar axis is reformed and becomes connected to the exit of the proton wire in the C_{TM} domain of the distal antiporter-like subunit (NuoL). During substrate release, all protons are ejected into the periplasmic space through the distal subunit, using those highly conserved Glu^{TM5}–Lys^{TM7} ionic pairs as stepping stones for proton translocation. Critically, breaking any part of this proton wire likely disrupts the proton efflux. The long cation pathway partially formed by the central polar axis appears to work reliably for protons which may use the hop-turn Grotthuss-type mechanism to move through a narrow path. However, it might to be more challenging for other cations such as Na^+ which require extensive coordination (Wraight 2006). Such structural difficulty would disappear if the distal antiporter-like subunit worked alone (Steuber 2003). The detailed mechanism of how proton loading in the C_{in} state triggers the neutralization of electrons in the redox center remains to be further investigated, though it is likely to be complex-specific, depending on the type of redox arm used. If injection of one pair of electrons is able to change the conformations of four proton pumps, it is also conceivable that loading of four substrate protons in the pumps promotes protonation in the Q-site by electrostatically inducing conformational changes at the redox center, *e.g.,* by modulating the Q^{2-}-binding pocket to a more hydrophilic environment (Efremov and Sazanov 2012).

A long-standing question in the field of Complex-I research remains as to why the Mrp antiporter-homologous cation pumps are often present in multiple copies, distinct from all other types of known transporters. Although the subunit interfaces have been suggested to be involved in substrate translocation (Sperling *et al.* 2016), the functional roles played by each subunit seem to be different (Morino *et al.* 2017). In our model, the distal subunit (NuoL) performs unique functions. While it seems to be able to function independently as a transporter (Steuber 2003), NuoL provides the only exit path for substrate protons from other proton-pumping subunits (NuoM, N, and possibly even the P_P-module) in an intact Complex-I. Moreover, protons released from other pumps may not pass through the entire central polar axis in one functional cycle. Instead, they may be temporarily stored in those intermediate proton buffer zones (*e.g.,* water clusters), traveling the proton wire in multiple steps in a manner of the Newton's cradle. According to this model, a more proximal antiporter-like subunit may only perform its pumping function when the central polar axis to its distal-side subunit is well formed. Otherwise, the C_{out} would appear to be a high-energy state, compared to the C_{in} state. This argument suggests sequential conformational changes propagating from the distal subunit to the proximal pump. At the end of the functional cycle, the C_{out} conformation at the most proximal, proton-pumping unit triggers the release of QH_2, permitting the start of the next cycle. Such cooperativity between proton-pumping subunits ensures both tight coupling between the redox reaction and proton pumping as well as high efficiency of energy conversion. Otherwise, if the pump subunits function independently, the tight coupling between each pulse of electron injection and conformational change in more distal pumps is not guaranteed.

In agreement with our model, experimental deletion of the distal subunit diminished the redox-enzyme activity of Complex-I. In addition, truncation/deletion of the NuoL subunit reducing the correct assembly of Complex-I (Belevich *et al.* 2011; Torres-Bacete *et al.* 2011) and softening the HL helix by inserting flexible peptides (*e.g.*, near the interface between NuoL and NuoM) result in de-coupling the proton translocation from the redox reaction (Belevich *et al.* 2011). Furthermore, certain activity-reducing point mutations of conserved acidic residues located in drastically different regions of NuoL result in loss of its sensitivity to the inhibitor 5-(*N*-ethyl-N-isopropyl)-amiloride (EIPA) in an

apparently similar way (Nakamaru-Ogiso *et al.* 2010). A possible explanation is that these mutations reduce the ability of NuoL to electrostatically responded to the electron injection, preventing domain repacking in NuoL and thus reducing sensitivity to EIPA which presumably binds preferentially to the excited C_{in} state of NuoL (but also see Murai *et al.* (2015)). Interestingly, this type of point mutations may not affect the export of protons from other subunits through the intact central polar axis. In agreement with this argument, the resultant Complex-I variants (with acidic to neutral mutations in NuoL) showed reduced but not abolished proton-pumping activity (*i.e.,* lowering the stoichiometric ratio of H^+/e^-) (Nakamaru-Ogiso *et al.* 2010). In addition, it was shown previously that removing of the distant subunits, ND5 and ND4 (homologous of NuoL and NuoM), in a yeast Complex-I is partially tolerable (Drose *et al.* 2011). In particular, in this variant the Q-reduction rate is lowered to $\sim$30% of the full complex, and the stoichiometric ratio of H^+/e^- is reduced to half, suggesting that the normal proton-exit path is disrupted. It is likely that truncation of the membrane arm forces formation of an alternative proton exit at the distal end of the arm, which becomes shorter, yet also more resistant to proton translocation.

In general, the number of antiporter-like subunits in the membrane arm must match the released energy from the redox center (Efremov and Sazanov 2012). For instance, the MBH complex contains only one antiporter-like subunit, an observation consistent with the fact that less energy is available from the corresponding redox reaction (Yu *et al.* 2018). On the one hand, if too many pumps are integrated in the membrane arm, the energy associated with the electron injection would be insufficient to drive conformational changes in all antiporter-like subunits. In such cases, not only the more distal pumps become malfunctioning, but also the entire Complex-I may not properly function. On the other hand, the counter-acting force from the pumps to the electrons (*i.e.,* the driving substance) determines whether the electron pair can be properly injected into the redox center. If for any reason the C_{out}-to-C_{in} conformational change in the pumps meets strong resistance, the electron injection will not be carried out, equivalent to lowering the midpoint redox potential of quinone. In such cases, the electron may even be rejected back from the ionized quinone (Q^{2-}) into the electron buffer zone in the redox arm, and thus the redox reaction be reversed. Consistent with this argument, the electron paramagnetic resonance (EPR) signal from semiquinone (SQ_{Nf}), an intermediate of the electron injection process, was found to be extremely sensitive to $\Delta\mu_{H+}$ applied across the mitochondrial inner membrane (Ohnishi *et al.* 2018). Furthermore, it is worth to point out that certain predictions from our current model are falsifiable experimentally. For instance, we predict that, by introducing a short circuit from the central polar axis to the periplasmic surface of the membrane in any pump subunit other than the distal one, efficiency of energy conversion in Complex-I will be lowered. More interestingly, in the context of such a mutant variant, a "detrimental" mutation in the distal pump may appear less severe on the redox activity and overall proton pumping.

Study on the proton-pumping mechanism of Complex-I is an intensively active research area. It is our hope that our model will provide a usable roadmap to the field to solve the seemingly mysterious mechanism of energy coupling in Complex-I.

Abbreviations

MBH	Membrane-bound hydrogenase
Mrp	Multiple resistance and pH-adaptation (cation/H^+ antiporters)
NADH	Nicotinamide adenine dinucleotide
Q	(ubi)quinone
TM	Transmembrane (helix)

Acknowledgements The authors thank Dr. Torsten Juelich (Peking University, China) for linguistic assistance during the preparation of this manuscript. This work was supported by National Natural Science Foundation of China (31470745), the Ministry of Science and Technology (China) (2015CB910104), and the Chinese Academy of Sciences (XDB08020301).

Compliance with Ethical Standards

Conflict of interest Xuejun C. Zhang and Bin Li declare that they have no conflict of interest.

Human and animal rights and informed consent This article does not contain any studies with human or animal subjects performed by any of the authors.

References

Abramson J, Smirnova I, Kasho V, Verner G, Kaback HR, Iwata S (2003) Structure and mechanism of the lactose permease of *Escherichia coli*. Science 301(5633):610–615

Amarneh B, Vik SB (2003) Mutagenesis of subunit N of the *Escherichia coli* complex I. Identification of the initiation codon and the sensitivity of mutants to decylubiquinone. Biochemistry 42(17):4800–4808

Babot M, Labarbuta P, Birch A, Kee S, Fuszard M, Botting CH, Wittig I, Heide H, Galkin A (2014) ND3, ND1 and 39 kDa subunits are more exposed in the de-active form of bovine mitochondrial complex I. Biochim Biophys Acta 1837(6):929–939

Baradaran R, Berrisford JM, Minhas GS, Sazanov LA (2013) Crystal structure of the entire respiratory complex I. Nature 494(7438):443–448

Belevich G, Knuuti J, Verkhovsky MI, Wikstrom M, Verkhovskaya M (2011) Probing the mechanistic role of the long alpha-helix in subunit L of respiratory Complex I from *Escherichia coli* by site-directed mutagenesis. Mol Microbiol 82(5):1086–1095

Brandt U (2011) A two-state stabilization-change mechanism for proton-pumping complex I. Biochim Biophys Acta 1807(10):1364–1369

Cabrera-Orefice A, Yoga EG, Wirth C, Siegmund K, Zwicker K, Guerrero-Castillo S, Zickermann V, Hunte C, Brandt U (2018) Locking loop movement in the ubiquinone pocket of complex I disengages the proton pumps. Nat Commun 9(1):4500

Carroll J, Fearnley IM, Skehel JM, Shannon RJ, Hirst J, Walker JE (2006) Bovine complex I is a complex of 45 different subunits. J Biol Chem 281(43):32724–32727

Cooley RB, Arp DJ, Karplus PA (2010) Evolutionary origin of a secondary structure: pi-helices as cryptic but widespread insertional variations of alpha-helices that enhance protein functionality. J Mol Biol 404(2):232–246

Dang S, Sun L, Huang Y, Lu F, Liu Y, Gong H, Wang J, Yan N (2010) Structure of a fucose transporter in an outward-open conformation. Nature 467(7316):734–738

Di Luca A, Gamiz-Hernandez AP, Kaila VRI (2017) Symmetry-related proton transfer pathways in respiratory complex I. Proc Natl Acad Sci USA 114(31):E6314–E6321

Drose S, Krack S, Sokolova L, Zwicker K, Barth HD, Morgner N, Heide H, Steger M, Nubel E, Zickermann V, Kerscher S, Brutschy B, Radermacher M, Brandt U (2011) Functional dissection of the proton pumping modules of mitochondrial complex I. PLoS Biol 9(8):e1001128

Dudkina NV, Kudryashev M, Stahlberg H, Boekema EJ (2011) Interaction of complexes I, III, and IV within the bovine respirasome by single particle cryoelectron tomography. Proc Natl Acad Sci USA 108(37):15196–15200

Efremov RG, Sazanov LA (2011) Structure of the membrane domain of respiratory complex I. Nature 476(7361):414–420

Efremov RG, Sazanov LA (2012) The coupling mechanism of respiratory complex I—a structural and evolutionary perspective. Biochim Biophys Acta 1817 10:1785–1795

Efremov RG, Baradaran R, Sazanov LA (2010) The architecture of respiratory complex I. Nature 465(7297):441–445

Euro L, Belevich G, Verkhovsky MI, Wikstrom M, Verkhovskaya M (2008) Conserved lysine residues of the membrane subunit NuoM are involved in energy conversion by the proton-pumping NADH:ubiquinone oxidoreductase (Complex I). Biochim Biophys Acta 1777(9):1166–1172

Fearnley IM, Walker JE (1992) Conservation of sequences of subunits of mitochondrial complex I and their relationships with other proteins. Biochim Biophys Acta 1140(2):105–134

Formosa LE, Dibley MG, Stroud DA, Ryan MT (2018) Building a complex complex: assembly of mitochondrial respiratory chain complex I. Semin Cell Dev Biol 76:154–162

Friedrich T, Scheide D (2000) The respiratory complex I of bacteria, archaea and eukarya and its module common with membrane-bound multisubunit hydrogenases. FEBS Lett 479(1–2):1–5

Friedrich T, Steinmuller K, Weiss H (1995) The proton-pumping respiratory complex I of bacteria and mitochondria and its homologue in chloroplasts. FEBS Lett 367(2):107–111

Galkin A, Meyer B, Wittig I, Karas M, Schagger H, Vinogradov A, Brandt U (2008) Identification of the mitochondrial ND3 subunit as a structural component involved in the active/deactive enzyme transition of respiratory complex I. J Biol Chem 283(30):20907–20913

Guenebaut V, Schlitt A, Weiss H, Leonard K, Friedrich T (1998) Consistent structure between bacterial and mitochondrial NADH:ubiquinone oxidoreductase (complex I). J Mol Biol 276(1):105–112

Hamamoto T, Hashimoto M, Hino M, Kitada M, Seto Y, Kudo T, Horikoshi K (1994) Characterization of a gene responsible for the Na^+/H^+ antiporter system of alkalophilic *Bacillus* species strain C-125. Mol Microbiol 14(5):939–946

Heng J, Zhao Y, Liu M, Liu Y, Fan J, Wang X, Zhang XC (2015) Substrate-bound structure of the *E. coli* multidrug resistance transporter MdfA. Cell Res 25(9):1060–1073

Hill TL (1989) Free energy transduction and biochemical cycle kineticsedn. Springer-Verlag, New York

Hirst J (2013) Mitochondrial complex I. Annu Rev Biochem 82:551–575

Huang Y, Lemieux MJ, Song J, Auer M, Wang DN (2003) Structure and mechanism of the glycerol-3-phosphate transporter from *Escherichia coli*. Science 301(5633):616–620

Jardetzky O (1966) Simple allosteric model for membrane pumps. Nature 211(5052):969–970

Jones AJ, Blaza JN, Varghese F, Hirst J (2017) Respiratory Complex I in *Bos taurus* and *Paracoccus denitrificans* pumps four protons across the membrane for every NADH oxidized. J Biol Chem 292(12):4987–4995

Kaila VRI (2018) Long-range proton-coupled electron transfer in biological energy conversion: towards mechanistic understanding of respiratory complex I. J R Soc Interface. https://doi.org/10.1098/rsif.2017.0916

Kaila VR, Wikstrom M, Hummer G (2014) Electrostatics, hydration, and proton transfer dynamics in the membrane domain of respiratory complex I. Proc Natl Acad Sci USA 111(19):6988–6993

Kotlyar AB, Sled VD, Vinogradov AD (1992) Effect of Ca^{2+} ions on the slow active/inactive transition of the mitochondrial NADH-ubiquinone reductase. Biochim Biophys Acta 1098(2):144–150

Morino M, Ogoda S, Krulwich TA, Ito M (2017) Differences in the phenotypic effects of mutations in homologous MrpA and MrpD subunits of the multi-subunit Mrp-type Na(+)/H(+) antiporter. Extremophiles 21(1):51–64

Murai M, Murakami S, Ito T, Miyoshi H (2015) Amilorides bind to the quinone binding pocket of bovine mitochondrial complex I. Biochemistry 54(17):2739–2746

Nakamaru-Ogiso E, Sakamoto K, Matsuno-Yagi A, Miyoshi H, Yagi T (2003) The ND5 subunit was labeled by a photoaffinity analogue of fenpyroximate in bovine mitochondrial complex I. Biochemistry 42(3):746–754

Nakamaru-Ogiso E, Kao MC, Chen H, Sinha SC, Yagi T, Ohnishi T (2010) The membrane subunit NuoL (ND5) is involved in the indirect proton pumping mechanism of *Escherichia coli* complex I. J Biol Chem 285(50):39070–39078

Ohnishi T, Ohnishi ST, Salerno JC (2018) Five decades of research on mitochondrial NADH-quinone oxidoreductase (complex I). Biol Chem 399(11):1249–1264

Parey K, Brandt U, Xie H, Mills DJ, Siegmund K, Vonck J, Kuhlbrandt W, Zickermann V (2018) Cryo-EM structure of respiratory complex I at work. Elife. https://doi.org/10.7554/eLife.39213

Pornillos O, Chang G (2006) Inverted repeat domains in membrane proteins. FEBS Lett 580(2):358–362

Roberts PG, Hirst J (2012) The deactive form of respiratory complex I from mammalian mitochondria is a Na^+/H^+ antiporter. J Biol Chem 287(41):34743–34751

Sazanov LA (2015) A giant molecular proton pump: structure and mechanism of respiratory complex I. Nat Rev Mol Cell Biol 16(6):375–388

Sazanov LA, Peak-Chew SY, Fearnley IM, Walker JE (2000) Resolution of the membrane domain of bovine complex I into subcomplexes: implications for the structural organization of the enzyme. Biochemistry 39(24):7229–7235

Schuller JM, Birrell JA, Tanaka H, Konuma T, Wulfhorst H, Cox N, Schuller SK, Thiemann J, Lubitz W, Setif P, Ikegami T, Engel BD, Kurisu G, Nowaczyk MM (2019) Structural adaptations of photosynthetic complex I enable ferredoxin-dependent electron transfer. Science 363(6424):257–260

Screpanti E, Hunte C (2007) Discontinuous membrane helices in transport proteins and their correlation with function. J Struct Biol 159(2):261–267

Shi Y (2013) Common folds and transport mechanisms of secondary active transporters. Annu Rev Biophys 42:51–72

Sperling E, Gorecki K, Drakenberg T, Hagerhall C (2016) Functional Differentiation of antiporter-like polypeptides in Complex I; a Site-directed mutagenesis study of residues conserved in MrpA and NuoL but not in MrpD, NuoM, and NuoN. PLoS One 11(7):e0158972

Steimle S, Schnick C, Burger EM, Nuber F, Kramer D, Dawitz H, Brander S, Matlosz B, Schafer J, Maurer K, Glessner U, Friedrich T (2015) Cysteine scanning reveals minor local rearrangements of the horizontal helix of respiratory complex I. Mol Microbiol 98(1):151–161

Steuber J (2003) The C-terminally truncated NuoL subunit (ND5 homologue) of the Na^+-dependent complex I from *Escherichia coli* transports Na^+. J Biol Chem 278(29):26817–26822

Torres-Bacete J, Nakamaru-Ogiso E, Matsuno-Yagi A, Yagi T (2007) Characterization of the NuoM (ND4) subunit in *Escherichia coli* NDH-1: conserved charged residues essential for energy-coupled activities. J Biol Chem 282(51):36914–36922

Torres-Bacete J, Sinha PK, Matsuno-Yagi A, Yagi T (2011) Structural contribution of C-terminal segments of NuoL (ND5) and NuoM (ND4) subunits of complex I from *Escherichia coli*. J Biol Chem 286(39):34007–34014

Verkhovskaya M, Bloch DA (2013) Energy-converting respiratory Complex I: on the way to the molecular mechanism of the proton pump. Int J Biochem Cell Biol 45(2):491–511

Verkhovskaya ML, Belevich N, Euro L, Wikstrom M, Verkhovsky MI (2008) Real-time electron transfer in respiratory complex I. Proc Natl Acad Sci USA 105(10):3763–3767

Vinogradov AD (1998) Catalytic properties of the mitochondrial NADH-ubiquinone oxidoreductase (complex I) and the pseudo-reversible active/inactive enzyme transition. Biochim Biophys Acta 1364(2):169–185

Walker JE (1992) The NADH:ubiquinone oxidoreductase (complex I) of respiratory chains. Q Rev Biophys 25(3):253–324

Weinert T, Skopintsev P, James D, Dworkowski F, Panepucci E, Kekilli D, Furrer A, Brunle S, Mous S, Ozerov D, Nogly P, Wang M, Standfuss J (2019) Proton uptake mechanism in bacteriorhodopsin captured by serial synchrotron crystallography. Science 365(6448):61–65

Wickstrand C, Dods R, Royant A, Neutze R (2015) Bacteriorhodopsin: would the real structural intermediates please stand up? Biochim Biophys Acta 1850 3:536–553

Wraight CA (2006) Chance and design–proton transfer in water, channels and bioenergetic proteins. Biochim Biophys Acta 1757(8):886–912

Yu H, Wu CH, Schut GJ, Haja DK, Zhao G, Peters JW, Adams MWW, Li H (2018) Structure of an ancient respiratory system. Cell 173(7):1636–1649

Zhang XC, Li H (2019) Interplay between the electrostatic membrane potential and conformational changes in membrane proteins. Protein Sci. https://doi.org/10.1002/pro.3563

Zhang XC, Zhao Y, Heng J, Jiang D (2015) Energy coupling mechanisms of MFS transporters. Protein Sci 24(10):1560–1579

Zhang XC, Liu M, Lu G, Heng J (2018a) Thermodynamic secrets of multidrug resistance: a new take on transport mechanisms of secondary active antiporters. Protein Sci 27(3):595–613

Zhang XC, Yang H, Liu Z, Sun F (2018b) Thermodynamics of voltage-gated ion channels. Biophys Rep 4(6):300–319

Zhu J, Vinothkumar KR, Hirst J (2016) Structure of mammalian respiratory complex I. Nature 536(7616):354–358

Zhu S, Vik SB (2015) Constraining the lateral helix of respiratory Complex I by cross-linking does not impair enzyme activity or proton translocation. J Biol Chem 290(34):20761–20773

Zickermann V, Wirth C, Nasiri H, Siegmund K, Schwalbe H, Hunte C, Brandt U (2015) Structural biology. Mechanistic insight from the crystal structure of mitochondrial complex I. Science 347(6217):44–49

